Check for updates

View Article Online
View Journal

PCCP

Accepted Manuscript

This article can be cited before page numbers have been issued, to do this please use: D. P. Malenov and S. D. Zaric, *Phys. Chem. Chem. Phys.*, 2018, DOI: 10.1039/C7CP06262A.

This is an Accepted Manuscript, which has been through the Royal Society of Chemistry peer review process and has been accepted for publication.

Accepted Manuscripts are published online shortly after acceptance, before technical editing, formatting and proof reading. Using this free service, authors can make their results available to the community, in citable form, before we publish the edited article. We will replace this Accepted Manuscript with the edited and formatted Advance Article as soon as it is available.

You can find more information about Accepted Manuscripts in the author guidelines.

Please note that technical editing may introduce minor changes to the text and/or graphics, which may alter content. The journal's standard Terms & Conditions and the ethical guidelines, outlined in our author and reviewer resource centre, still apply. In no event shall the Royal Society of Chemistry be held responsible for any errors or omissions in this Accepted Manuscript or any consequences arising from the use of any information it contains.

ROYAL SOCIETY OF CHEMISTRY

rsc.li/pccp

Please do not adjust margins
View Article Online
DOI: 10.1039/C7CP06262A

PCCP

ARTICLE

Chelated metal ion modulates the strength and geometry of stacking interactions: energies and potential energy surfaces for chelate-chelate stacking

Received 00th January 20xx,
Accepted 00th January 20xx

DOI: 10.1039/x0xx00000x

www.rsc.org/

D. P. Malenov[a] and S. D. Zarić*[a,b]

Quantum chemical calculations were performed on model systems of stacking interactions between the *acac* type chelate rings of nickel, palladium, and platinum. The CCSD(T)/CBS calculations showed that chelate-chelate stacking interactions are significantly stronger than chelate-aryl and aryl-aryl stacking interactions. Interaction energy surfaces were calculated at LC-ωPBE-D3BJ/aug-cc-pVDZ level, which gives energies in good agreement with CCSD(T)/CBS. Stacking of chelates in antiparallel orientation is stronger than stacking in parallel orientation, which is in agreement with larger number of antiparallel stacked chelates in the CSD crystal structures. The strongest antiparallel chelate-chelate stacking interaction is formed between two platinum chelates, with CCSD(T)/CBS interaction energy of -9.70 kcal/mol, while the strongest stacking between two palladium chelates and two nickel chelates has CCSD(T)/CBS energies of -9.21 kcal/mol and -9.50 kcal/mol, respectively. The strongest parallel chelate-chelate stacking was found for palladium chelates, with LC-ωPBE-D3BJ/aug-cc-pVDZ energy of -6.51 kcal/mol. The geometries of potential surface minima are not the same for the three metals. The geometries of minima are governed by electrostatic interactions, which are the ones determining the positions of energy minima. Electrostatic interactions are governed by different electrostatic potentials above the metals, which is very positive for nickel, slightly positive for palladium, and slightly negative for platinum.

Introduction

Stacking interactions are of great importance for various chemical and biological systems.[1] Most of the studies on stacking interactions were dealing with aromatic molecules,[2–11] primarily due to their significant role for protein[12,13] and DNA structure.[14,15] However, in the past decade it was shown in numerous studies that other molecules and fragments can be involved in stacking interactions.[16–21] Moreover, it was shown that stacking interactions that involve nonaromatic rings or molecules have similar or even higher energies than aromatic stacking interactions.[20,22–24]

It has been shown that chelate rings of transition metals, which are of great interest to materials science[25–27] and crystal engineering,[28–30] can also form stacking interactions.[16,17,31–34] Interactions of planar chelate rings with C_6 aromatic rings[16] and with other chelate rings[17] can be frequently found in crystal structures. It was shown that C_6 aromatic rings prefer stacking with chelate rings than with other C_6 aromatic rings, with geometries of these chelate-aryl stacking interactions being parallel displaced, similar to the geometries of aryl-aryl stacking interactions.[16] This preference of aromatic rings towards chelate rings was confirmed by calculating the interaction energies between benzene and six-membered chelate rings,[23,24] showing that chelate-benzene stacking can be substantially stronger (the strongest interaction has the energy of -6.39 kcal/mol)[24] than benzene-benzene stacking (-2.73 kcal/mol).[7]

The evidence of stacking interactions between two chelate rings was provided in several studies.[17,35–37] The analysis of crystal structures deposited in the Cambridge Structural Database showed high occurrence of stacking interactions between chelates fused with other chelate or aromatic rings, but also significant number of interactions between isolated chelate rings.[17] Geometries of these interactions can be parallel displaced (similar to geometries of aryl-aryl stacking interactions), with typical orientations of such rings being parallel and antiparallel, but they can also be face-to-face,[17,38] which is not typical for aryl-aryl stacking.[9]

There were several studies that attempted to quantify the strength of intermolecular interactions of complexes with chelate rings, however, the interactions were not only stacking of chelate rings, but they involved simultaneously other interaction types, such as hydrogen bonds.[22,38] In this study, we provide the first report on isolated chelate-chelate stacking interaction energies calculated with CCSD(T) method at the complete basis set (CBS), which is considered the gold standard of quantum chemistry.[39,40] Preliminary data on potential energy surfaces for chelate-chelate stacking interactions were published in a recent review.[41] In this paper, we provide the detailed study of potential energy surfaces of

[a] Faculty of Chemistry, University of Belgrade, Studentski trg 12-16, Belgrade, Serbia. E-mail: szaric@chem.bg.ac.rs
[b] Department of Chemistry, Texas A&M University at Qatar, P. O. Box 23874, Doha, Qatar.

Published on 01 May 2018. Downloaded by University of New England on 01/05/2018 12:59:59.

Physical Chemistry Chemical Physics Accepted Manuscript

View Article Online
DOI: 10.1039/C7CP06262A

Published on 01 May 2018. Downloaded by University of New England on 01/05/2018 12:59:59.

chelate-chelate stacking, followed by the analysis of electrostatic potentials to demonstrate the metal ion influence on these interactions.

Computational Details

All calculations were performed by using the Gaussian 09 (version D.01) program package.[42] Stacking interactions between chelate rings were studied on model molecules which contain nickel, palladium and platinum as metal ions. Ligands in these complexes are the formate anion (HCO_2^-), which forms four-membered chelate ring, and the enolate form of malondialdehyde ($C_3H_3O_2^-$), which forms six-membered chelate ring of *acetylacetonato* (*acac*) type, which is of our primary interest. Monomer geometries were optimized with M06HF density functional[43,44] with def2-TZVP basis set[45] and confirmed as true minima by performing calculations of vibrational frequencies. Effective core potentials were used for palladium and platinum atoms.[46]

To study chelate-chelate stacking, two orientations of chelate rings were considered: antiparallel and parallel (Figure 1), since these are the highly dominant orientations of chelate rings in crystal structures.[17]

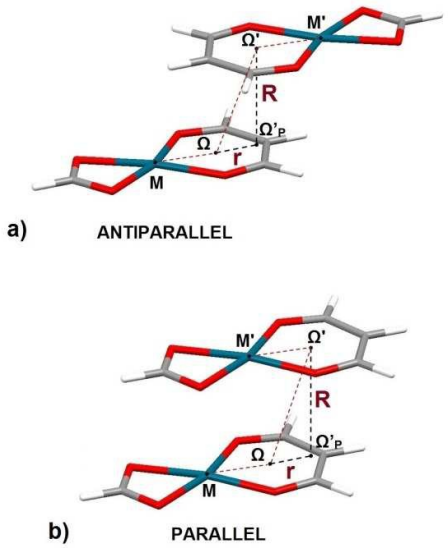

Figure 1. Geometrical parameters used for the description of chelate-chelate interactions. Centrers of interacting chelates are denotes as Ω and Ω', while Ω'_p is the projection of Ω' onto the plane of the other chelate. Normal distance R is the distance between Ω' and Ω'_p. Horizontal displacement (offset) r is the distance from the Ω to Ω'_p. If torsion angle M-Ω-Ω'-M' is equal to 180°, the interacting chelates are in antiparallel orientation (a); it torsion angle M-Ω-Ω'-M' is equal to 0°, the interacting chelates are in parallel orientation (b).

Potential energy surfaces for stacking of nickel, palladium and platinum chelates were therefore calculated with LC-ωPBE density functional[47–49] with Grimme D3 dispersion correction and Becke Johnson damping (D3BJ),[50] by using the aug-cc-pVDZ basis set.[51–55] Effective core potentials were used for palladium and platinum atoms.[46] Basis set superposition error was removed by counterpoise procedure of Boys and Bernardi.[56] We used this method, since we have shown that it is in good agreement with CCSD(T)/CBS level (see Supporting Information). The CCSD(T)/CBS energies were calculated for minima at potential energy surfaces, using the method of Mackie and DiLabio.[57]

Electrostatic potential maps for the complexes of nickel, palladium and platinum from our previous work[41] were used in this study to explain the electrostatic effects in chelate-chelate stacks. These maps were calculated from LC-ωPBE-D3BJ/aug-cc-pVDZ wave functions obtained with Gaussian 09 suites of programs, and visualized with gOpenMol v3.0 program.[58] The surfaces of all three molecules were defined by 0.004 a.u. contour of electron density, since it was shown previously that the differences on electrostatic potential surfaces of complexes with different metals can be noticed at this value.[59]

Results and Discussion

Interaction energies and potential energy surfaces

Potential energy surfaces were calculated at LC-ωPBE-D3BJ/aug-cc-pVDZ level for model systems of nickel, palladium and platinum complexes presented at Figures 2 and 3. Potential energy surfaces were calculated by varying the normal distances for the series of offset values (Figure 1). The strongest calculated energies for all offset values are presented as potential energy curves (Figures 4 and 6).

The starting position for both antiparallel and parallel orientations is *face-to-face*, with center of one *acac* type chelate above the center of the other *acac* type chelate ring (geometries $\mathbf{0_{ap}}$ and $\mathbf{0_p}$, Figures 2 and 3, respectively). The position of one chelate ring was then fixed, while the other one was displaced in different directions (Figures 2 and 3): along the twofold axis (model systems $\mathbf{A_{ap}}$ and $\mathbf{A_p}$) and along the line normal to the axis (model systems $\mathbf{B_{ap}}$ and $\mathbf{B_p}$). For antiparallel orientation, two different directions of displacement are possible; hence two subsystems are distinguished, with positive and negative offsets (Figure 2). Additional model system, which considers the displacement along the line forming 45° angle with the C_2 axis (model systems $\mathbf{AB_{ap}}$ and $\mathbf{AB_p}$) is presented in Supporting Information. Preliminary results for model systems $\mathbf{A_{ap}}$ and $\mathbf{A_p}$ were published in a recent review,[41] while here they are completed and broadened by including the other model systems.

Physical Chemistry Chemical Physics Accepted Manuscript

This journal is © The Royal Society of Chemistry 20xx

View Article Online
DOI: 10.1039/C7CP06262A

Published on 01 May 2018. Downloaded by University of New England on 01/05/2018 12:59:59.

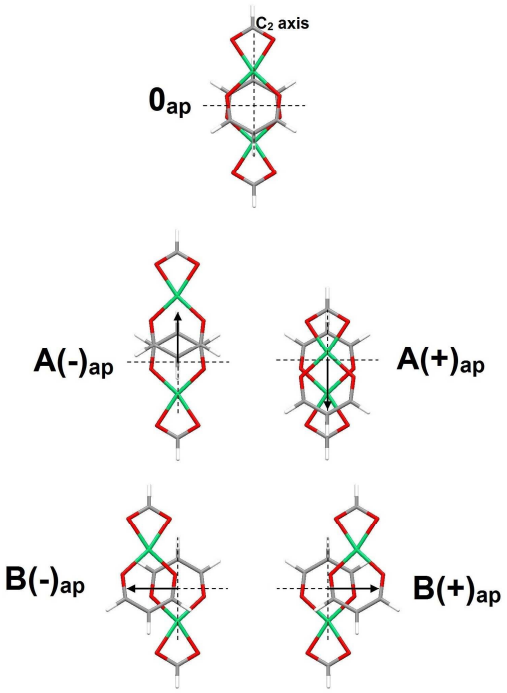

Figure 2. Model systems for calculations of chelate-chelate stacking potential surfaces for antiparallel orientation. Model systems $B(-)_{ap}$ and $B(+)_{ap}$ are equivalent

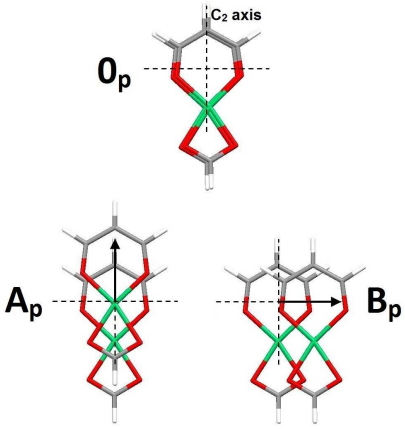

Figure 3. Model systems for calculations of chelate-chelate stacking potential surfaces for parallel orientation

Data in Figures 4 and 6, as well as data in Tables 1 and 2, indicate that antiparallel chelate-chelate stacking is stronger than parallel, what is in accordance with larger number of antiparallel stacked chelates in the CSD crystal structures.[17,41] The chelate-chelate stacking for all three metals is the strongest in the model system A_{ap}.

For antiparallel model system, the shapes of potential energy curves A_{ap} are not similar for nickel, palladium and platinum chelates (Figure 4). For nickel chelate-chelate stacking, minimum on A_{ap} curve appears at r = 0.6 Å (Figure 4 and 5), with CCSD(T)/CBS interaction energy of -9.50 kcal/mol (Table 1). This is the strongest interaction between nickel chelates found in this study. Minima for palladium and platinum chelates are at r = 2.7 Å (Figure 4 and 5), with CCSD(T)/CBS interaction energy of -9.21 kcal/mol, and -9.70 kcal/mol, respectively (Table 1). These are the strongest chelate-chelate stacking interactions for palladium and platinum chelates found in this study. Also, these data show that platinum chelates form the strongest stacking interaction (Table 1). The results also indicate that chelate-chelate stacking is stronger than aryl-aryl stacking (-2.73 kcal/mol)[7] and chelate-aryl stacking (-6.39 kcal/mol).[24]

In the offset region from -0.9 Å to 3.0 Å the A_{ap} curves are very different (Figure 4), suggesting the strong influence of metal ions (Figure 2). At other offsets, where influence of metal is not strong, the A_{ap} curves are of similar shape for all metals, with platinum chelate-chelate stacking being the strongest and nickel chelate-chelate stacking being the weakest.

At B_{ap} curves, the starting geometry (**0_{ap}**, Figure 5) is the minimum for all the metals (**B_{ap} min**, Figure 4). The strongest chelate-chelate stacking at B_{ap} curve is found for nickel chelates (the LC-ωPBE-D3BJ/aug-cc-pVDZ interaction energy is -8.98 kcal/mol, Table 1). At very small offsets, platinum chelate-chelate stacking is the weakest, however, at offsets larger than 1.2 Å, it is the strongest (Figure 4). Interestingly, at B_{ap} curve interactions start getting stronger at offsets larger than 4.2 Å (Figure 4), where molecules do not overlap anymore. This is, however, attributed to double C-H/O interactions, not to chelate-chelate stacking.

Table 1. Interaction energies (in kcal/mol) for the chelate-chelate stacking geometries in antiparallel orientation (Figure 5) calculated at LC-ωPBE-D3BJ/aug-cc-pVDZ level, with CCSD(T)/CBS level for the selected geometries.

ANTIPARALLEL	offset [Å]	INTERACTION ENERGY					
		LC-ωPBE-D3BJ/aug-cc-pVDZ			CCSD(T)/CBS		
		Ni	Pd	Pt	Ni	Pd	Pt
0_{ap} (B_{ap} min)	0.0	-8.98	-8.73	-8.05	-	-	-
A_{ap} 0.6	0.6	-9.42	-9.05	-8.31	-9.50	-8.86	-8.10
A_{ap} 2.7	2.7	-7.71	-9.30	-9.73	-7.83	-9.21	-9.70

Physical Chemistry Chemical Physics Accepted Manuscript

View Article Online
DOI: 10.1039/C7CP06262A

Published on 01 May 2018. Downloaded by University of New England on 01/05/2018 12:59:59.

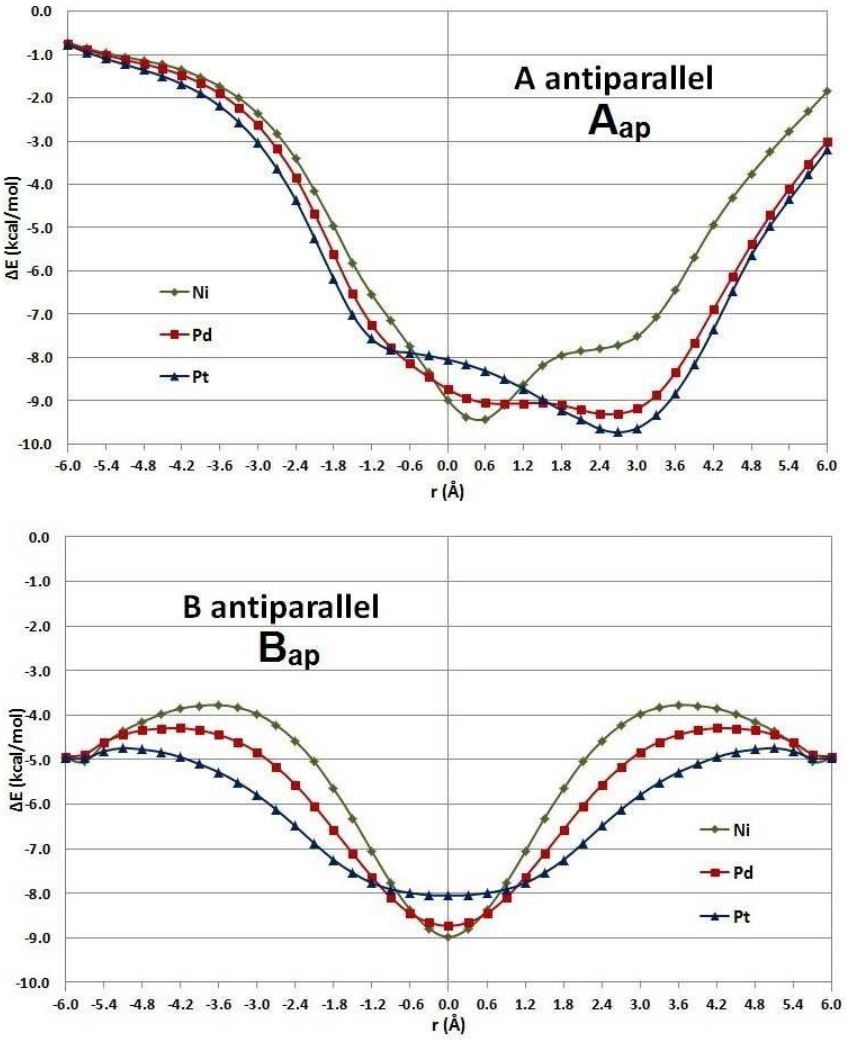

Figure 4. Potential energy curves for chelate-chelate stacking in antiparallel orientation for model systems A and B, calculated at LC-ωPBE-D3BJ/aug-cc-pVDZ level. Normal distances were varied for each offset value in a series of single point calculations; the curve presents the energy of the strongest interaction for each offset.

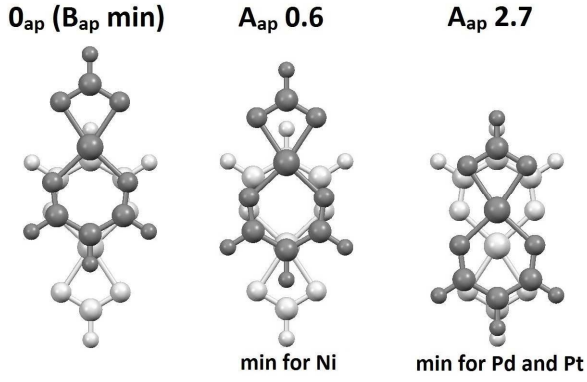

Figure 5. Geometries of energy minima on potential energy curves (Figure 4) for chelate-chelate stacking in antiparallel orientation.

Parallel chelate-chelate stacking for different metals shows more similar curves than antiparallel stacking (Figure 6). For parallel orientations (Figure 3 and 6) chelate-chelate stacking minimum at Ap curve is the strongest for platinum, while for palladium and nickel, minima at Bp curves are the strongest (Table 2). The strongest chelate-chelate stacking in parallel orientation is **B_p min** for palladium (Figure 7) with interaction energy of -6.51 kcal/mol (Table 2).

The A_p curves show that the strongest stacking was found for platinum chelates. The platinum **A_p min** is at r = 1.5 Å (Figure 7), with interaction energy of -6.28 kcal/mol (Table 2). The palladium **A_p min** is at r = 1.8 Å with interaction energy of -5.97 kcal/mol (Table 2). The A_p curves for palladium and platinum in the offset range from 3.3 Å to 4.2 Å are very flat (Figure 6), due to the overlaying of six-membered and four-membered chelate ring (Figure 3).

The A_p curve for nickel shows the minimum at r = 1.8 Å (Figure 6), but with significantly weaker stacking, interaction

Physical Chemistry Chemical Physics Accepted Manuscript

View Article Online
DOI: 10.1039/C7CP06262A

Published on 01 May 2018. Downloaded by University of New England on 01/05/2018 12:59:59.

energy is -4.80 kcal/mol, Table 2. However, at the area of overlapping of six-membered and four-membered chelates of nickel, new minimum appears at r = 3.6 Å (Figure 6), with somewhat stronger interaction energy of -5.03 kcal/mol.

As was mentioned above, for nickel and palladium parallel orientation stacking is strongest in B_p orientation (Figure 6, Table 2). The **B_p min** for palladium and nickel are found at r = 1.8 Å (Figure 7), with interaction energies of -6.51 kcal/mol and -5.74 kcal/mol, respectively (Table 2). For platinum, the minimum on B_p curve is at r = 1.5 Å, with interaction energy of -6.19 kcal/mol (Table 2), which is somewhat weaker than platinum **A_p min** (-6.28 kcal/mol, Table 2).

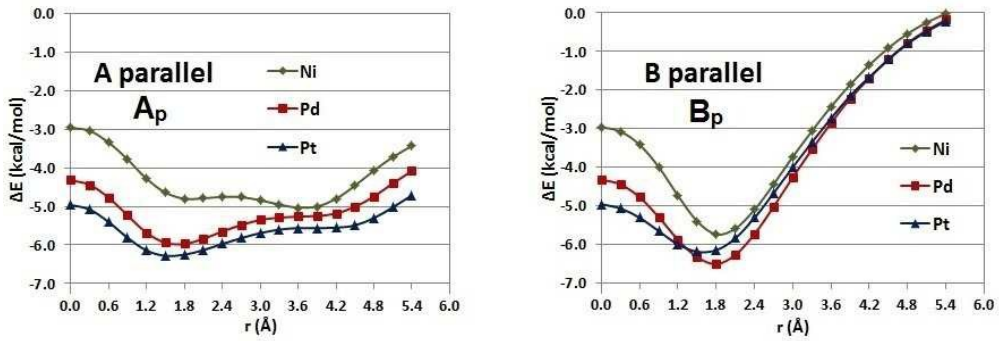

Figure 6. Potential energy curves for chelate-chelate stacking in parallel orientation for model systems A and B, calculated at LC-ωPBE-D3BJ/aug-cc-pVDZ level. Normal distances were varied for each offset value in a series of single point calculations; the curve presents the energy of the strongest interaction for each offset.

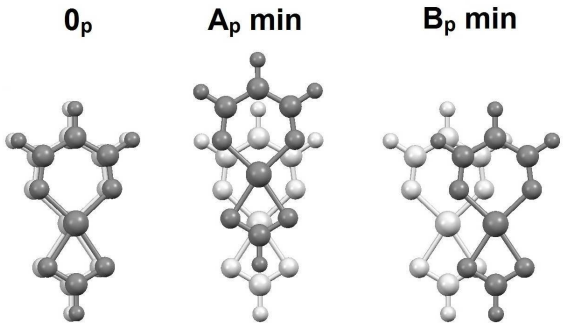

Figure 7. Geometries of energy minima on potential energy curves (Figure 6) for chelate-chelate stacking in parallel orientation. The offsets for A_p min and B_p min geometries are 1.8 Å for nickel and palladium chelates, and 1.5 Å for platinum chelates.

Overall, parallel chelate-chelate stacking (Table 2) is significantly weaker than antiparallel chelate-chelate stacking (Table 1). While the geometries of minima for nickel, palladium and platinum chelates are very different in antiparallel orientation (**A_{ap} 0.6** for Ni, **A_{ap} 2.7** for Pd and Pt, Figure 6), the geometries of minima in parallel orientation for these metals are very similar (Figure 8). The strongest antiparallel chelate-chelate stacking is the one between platinum chelates, while the strongest parallel chelate-chelate stacking is between palladium chelates (Tables 1 and 2). Additionally, antiparallel chelate-chelate stacking is the strongest when chelates are displaces along the twofold symmetry axis (orientation A_{ap}), while parallel chelate-chelate stacking is the strongest in perpendicular direction (orientation B_p).

The stacking in additional antiparallel (**AB_{ap}**) and parallel orientations (**AB_p**) (Figure S2, Supporting Information) is weaker than in antiparallel orientations **A_{ap}** and parallel **B_p**. The energy in antiparallel **AB_{ap}** orientation exceeds -9.0 kcal/mol only for nickel chelates, while in parallel orientation does not exceed -6.0 kcal/mol for none of the metals (Table S2).

Table 2. Interaction energies (in kcal/mol) for the chelate-chelate stacking geometries in parallel orientation (Figure 7) calculated at LC-ωPBE-D3BJ/aug-cc-pVDZ level, with CCSD(T)/CBS energies for the selected geometries.

PARALLEL	offset [Å]			INTERACTION ENERGY LC-ωPBE-D3BJ/aug-cc-pVDZ			CCSD(T)/CBS		
	Ni	Pd	Pt	Ni	Pd	Pt	Ni	Pd	Pt
0_p (B_p max)	0.0	0.0	0.0	-2.96	-4.32	-4.96	-	-	-
A_p min	1.8	1.8	1.5	-4.80	-5.97	-6.28	-4.84	-5.82	-6.35
B_p min	1.8	1.8	1.5	-5.74	-6.51	-6.19	-	-	-

Physical Chemistry Chemical Physics Accepted Manuscript

View Article Online
DOI: 10.1039/C7CP06262A
ARTICLE PCCP

Published on 01 May 2018. Downloaded by University of New England on 01/05/2018 12:59:59.

Electrostatic Potential Maps

The apparently different stacking energies and preferences of chelates of nickel, palladium and platinum towards certain stacking offsets (Figures 4-7, Tables 1 and 2) can be rationalized by their electrostatic potential maps (Figure 8). Significant differences among electrostatic potential maps of the chelate complexes of the three metals exist. Electrostatic potentials above the metals are very different: very positive above nickel, slightly positive above palladium and slightly negative above palladium (Figure 8).

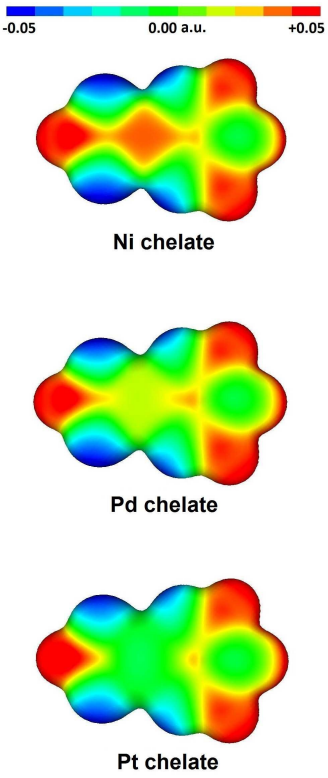

Figure 8. Electrostatic Potential maps for complexes containing chelate rings, at the surfaces defined by the 0.004 $e^-/Å^3$ contour of electron density. The data for plotting of the maps was taken from our previous work.[41]

In **A_{ap} 0.6** geometry (Figure 5), C1 and C3 atoms of one chelate are above oxygen atoms of the other chelate. Because of the opposite potentials around these atoms (positive around C1 and C3 and negative around oxygen, Figure 8) it leads to electrostatic attraction. Simultaneously, slightly negative area around the C2 atom of one chelate is above the metal of the other chelate. Different potentials around metal atoms for the three metals (Figure 8) make difference in this geometry. For nickel chelate, this electrostatic interaction is attractive, since electrostatic potential above nickel is very positive. For palladium chelate, electrostatic interaction is somewhat less attractive, since the potential above palladium is only slightly positive. For platinum chelate, electrostatic interaction is repulsive since the potential above platinum is slightly negative. Probably the most favorable electrostatic attraction between nickel chelates leads to **Ni A_{ap} 0.6** being the energy minimum and the strongest calculated stacking of nickel chelates (Figure 4, Table 1).

In **A_{ap} 2.7** geometry (Figure 5), slightly negative potential of C2 atom of *acac* type chelate is located above very positive potential above C atom of four-membered chelate (Figure 8), leading to electrostatic attraction. Simultaneously, positive electrostatic potential above one chelate center is located above the metal area of the other chelate. Since the potential above nickel is also positive (Figure 8), the electrostatic attraction for nickel chelates in **A_{ap} 2.7** should not be very favorable. More favorable attraction could be found for palladium chelates, since potential above palladium is significantly less positive than above nickel. The most favorable electrostatic attraction can be expected between platinum chelates, due to negative potential above platinum overlapping with positive potential above chelate center (Figure S7). The favorable electrostatic interactions for palladium and platinum chelates cause **A_{ap} 2.7** geometry to be the energy minimum for these two metals (Figure 4).

Parallel chelate-chelate stacking is weaker than antiparallel chelate-chelate stacking, since electrostatic interactions are not very favorable due to partial overlaying of the areas of the same electrostatic potentials (Figure 7). However, in **A_p min** parallel geometry metal area of one chelate is above the positive center of the other chelate (Figures 7 and S8). Since electrostatic potentials above platinum are slightly negative (Figure 8), there is electrostatic attraction with positive chelate center, causing **Pt A_p min** to be the strongest parallel platinum chelate-chelate stacking found in this study (Table 2). Potential above nickel and palladium chelate is positive, causing the electrostatic repulsion, with positive potential above the center of the other chelate in this geometry (Figure S8).

The **B_p min** geometry is not very stable for platinum. In these geometry, the area above metal of one chelate is in contact with the area above oxygen of the other chelate (Figure 7). In platinum complex, negative potentials around platinum causes repulsion with negative potentials around oxygen atoms. More favorable parallel chelate-chelate stacking of nickel and palladium chelates is found in **B_p min** geometries (Table 2). Since potential above nickel is very positive, attractive electrostatic interaction occurs with negative oxygens, making **Ni B_p min** geometry the one with the most stable parallel nickel chelate-chelate stacking (Table 2). Slightly positive palladium and negative oxygen produce only slight electrostatic attraction. However, **Pd B_p min** geometry has the strongest stacking of any chelates in parallel orientation found in this study. It is probably the consequence of stronger dispersion interactions for palladium (4d metal) than for nickel (3d metal) chelates.

Conclusions

Chelate-chelate stacking interactions of *acac* type chelates of nickel, palladium and platinum were studied by using quantum chemical methods. The calculated interaction energies at

Physical Chemistry Chemical Physics Accepted Manuscript

View Article Online
DOI: 10.1039/C7CP06262A

Published on 01 May 2018. Downloaded by University of New England on 01/05/2018 12:59:59.

CCSD(T)/CBS level showed that chelate-chelate stacking is significantly stronger than corresponding chelate-aryl[27] and aryl-aryl stacking.[7]

The results show that stacking of chelates in antiparallel orientation is stronger than stacking of chelates in parallel orientation, due to electrostatic attraction of antiparallel oriented chelates and electrostatic repulsion of parallel oriented chelates. These results are in agreement with the CSD studies, which show the preference for antiparallel orientation of stacked chelates.[17,41] The strongest stacking is found for platinum chelates, with CCSD(T)/CBS interaction energy of -9.70 kcal/mol, with palladium and nickel chelate-chelate stacking being somewhat weaker, with interaction energies of -9.21 kcal/mol and -9.50 kcal/mol. However, while the geometries of the strongest chelate-chelate stacking of palladium and platinum chelates are similar, the geometry of the strongest stacking of nickel chelates is different. Different geometries of energy minima for nickel, palladium and platinum chelates are the consequence of their electrostatic potentials, which are very positive above nickel atom, slightly positive above palladium and slightly negative above platinum atom. This study shows significant strength of chelate-chelate stacking interactions, with special emphasis on metal influence, on both their energies and geometries.

Acknowledgements

This work was supported by the Serbian Ministry of Education, Science and Technological Development (Grant 172065). The HPC resources and services used in this work were partially provided by the IT Research Computing group in Texas A&M University at Qatar. IT Research Computing is funded by the Qatar Foundation for Education, Science and Community Development (http://www.qf.org.qa).

References

1 L. M. Salonen, M. Ellermann and F. Diederich, *Angew. Chemie - Int. Ed.*, 2011, **50**, 4808–4842.
2 H. J. Schneider, *Angew. Chemie - Int. Ed.*, 2009, **48**, 3924–3977.
3 S. Grimme, *Angew. Chemie - Int. Ed.*, 2008, **47**, 3430–3434.
4 J. Sponer, K. E. Riley and P. Hobza, *Phys. Chem. Chem. Phys.*, 2008, **10**, 2595–2610.
5 M. Watt, L. K. E. Hardebeck, C. C. Kirkpatrick and M. Lewis, *J. Am. Chem. Soc.*, 2011, **133**, 3854–3862.
6 A. I. Anzellotti, C. A. Bayse and N. P. Farrell, *Inorg. Chem.*, 2008, **47**, 10425–10431.
7 E. C. Lee, D. Kim, P. Jurečka, P. Tarakeshwar, P. Hobza and K. S. Kim, *J. Phys. Chem. A*, 2007, **111**, 3446–3457.
8 C. Janiak, *Dalton Trans.*, 2000, **95**, 3885–3896.
9 D. B. Ninković, G. V. Janjić, D. Ž. Veljković, D. N. Sredojević and S. D. Zarić, *ChemPhysChem*, 2011, **12**, 3511–3514.
10 D. B. Ninković, J. M. Andrić, S. N. Malkov and S. D. Zarić, *Phys. Chem. Chem. Phys.*, 2014, **16**, 11173–7.
11 K. M. Langner, W. A. Sokalski and J. Leszczynski, *J. Chem. Phys.*, 2007, **127**, 111102.
12 S. Burley and G. Petsko, *Science*, 1985, **229**, 23–28.
13 P. Chakrabarti and U. Samanta, *J. Mol. Biol.*, 1995, **251**, 9–14.
14 C. A. Hunter and J. K. M. Sanders, *J. Am. Chem. Soc.*, 1990, **112**, 5525–5534.
15 V. L. Malinovskii, F. Samain and R. Häner, *Angew. Chemie Int. Ed.*, 2007, **46**, 4464–4467.
16 Z. D. Tomić, D. Sredojević and S. D. Zarić, *Cryst. Growth Des.*, 2006, **6**, 29–31.
17 D. N. Sredojević, Z. D. Tomić and S. D. Zarić, *Cryst. Growth Des.*, 2010, **10**, 3901–3908.
18 K. F. Konidaris, C. N. Morrison, J. G. Servetas, M. Haukka, Y. Lan, A. K. Powell, J. C. Plakatouras and G. E. Kostakis, *CrystEngComm*, 2012, **14**, 1842.
19 E. R. T. Tiekink, *Chem. Commun.*, 2014, **50**, 11079.
20 J. P. Blagojević and S. D. Zarić, *Chem. Commun.*, 2015, **51**, 12989–12991.
21 E. R. T. Tiekink, *Coord. Chem. Rev.*, 2017, **345**, 209–228.
22 K. F. Konidaris, A. C. Tsipis and G. E. Kostakis, *Chempluschem*, 2012, **77**, 354–360.
23 D. P. Malenov, D. B. Ninković and S. D. Zarić, *ChemPhysChem*, 2015, **16**, 761–768.
24 D. P. Malenov, D. B. Ninković, D. N. Sredojević and S. D. Zarić, *ChemPhysChem*, 2014, **15**, 2458–2461.
25 E. Coronado and P. Day, *Chem. Rev.*, 2004, **104**, 5419–5448.
26 N. Robertson and L. Cronin, *Coord. Chem. Rev.*, 2002, **227**, 93–127.
27 B. Bräuer, D. R. T. Zahn, T. Rüffer and G. Salvan, *Chem. Phys. Lett.*, 2006, **432**, 226–229.
28 T. S. Basu Baul, S. Kundu, S. Mitra, H. Höpfl, E. R. T. Tiekink and A. Linden, *Dalton Trans.*, 2013, **42**, 1905–20.
29 X. J. Wang, H. X. Jian, Z. P. Liu, Q. L. Ni, L. C. Gui and L. H. Tang, *Polyhedron*, 2008, **27**, 2634–2642.
30 D. Biswas, P. P. Chakrabarty, S. Saha, A. D. Jana, D. Schollmeyer and S. García-Granda, *Inorganica Chim. Acta*, 2013, **408**, 172–180.
31 F. A. Afkhami, A. A. Khandar, G. Mahmoudi, W. Maniukiewicz, A. V. Gurbanov, F. I. Zubkov, O. Şahin, O. Z. Yesilel, A. Frontera, A. Ienco, A. Frontera and M. S. Gargari, *CrystEngComm*, 2017, **19**, 1389–1399.
32 G. Mahmoudi, A. Castiñeiras, P. Garczarek, A. Bauzá, A. L. Rheingold, V. Kinzhybalo and A. Frontera, *CrystEngComm*, 2016, **18**, 1009–1023.
33 G. Mahmoudi, A. Bauza, A. V Gurbanov, F. I. Zubkov, W. Maniukiewicz, A. Rodriguez-Dieguez, E. Lopez-Torres and A. Frontera, *CrystEngComm*, 2016, **18**, 9056–9066.
34 N. A. M. S. Caturello, Z. Csók, G. Fernández and R. Q. Albuquerque, *Chem. - A Eur. J.*, 2016, **22**, 17681–17689.
35 K. F. Konidaris, A. K. Powell and G. E. Kostakis, *CrystEngComm*, 2011, **13**, 5872.
36 L. Holland, W.-Z. Shen, P. von Grebe, P. J. Sanz Miguel, F. Pichierri, A. Springer, C. A. Schalley and B. Lippert, *Dalton Trans.*, 2011, **40**, 5159–5161.
37 E. Laurila, L. Oresmaa, M. Niskanen, P. Hirva and M. Haukka, *Cryst. Growth Des.*, 2010, **10**, 3775–3786.

Physical Chemistry Chemical Physics Accepted Manuscript

View Article Online
DOI: 10.1039/C7CP06262A

38 S. Bhattacharya, S. Roy, K. Harms, A. Bauza, A. Frontera and S. Chattopadhyay, *Inorganica Chim. Acta*, 2016, **442**, 16–23.
39 M. O. Sinnokrot, E. F. Valeev and C. D. Sherrill, *J. Am. Chem. Soc.*, 2002, **124**, 10887–10893.
40 M. O. Sinnokrot and C. D. Sherrill, *J. Phys. Chem. A*, 2004, **108**, 10200–10207.
41 D. P. Malenov, G. V. Janjić, V. B. Medaković, M. B. Hall and S. D. Zarić, *Coord. Chem. Rev.*, 2017, **345**, 318–341.
42 M. J. Frisch, G. W. Trucks, H. B. Schlegel, G. E. Scuseria, M. A. Robb, J. R. Cheeseman, G. Scalmani, V. Barone, G. A. Petersson, H. Nakatsuji, X. Li, M. Caricato, A. Marenich, J. Bloino, B. G. Janesko, R. Gomperts, B. Mennucci, H. P. Hratchian, J. V. Ortiz, A. F. Izmaylov, J. L. Sonnenberg, D. Williams-Young, F. Ding, F. Lipparini, F. Egidi, J. Goings, B. Peng, A. Petrone, T. Henderson, D. Ranasinghe, V. G. Zakrzewski, J. Gao, N. Rega, G. Zheng, W. Liang, M. Hada, M. Ehara, K. Toyota, R. Fukuda, J. Hasegawa, M. Ishida, T. Nakajima, Y. Honda, O. Kitao, H. Nakai, T. Vreven, K. Throssell, J. A. Montgomery Jr., J. E. Peralta, F. Ogliaro, M. Bearpark, J. J. Heyd, E. Brothers, K. N. Kudin, V. N. Staroverov, T. Keith, R. Kobayashi, J. Normand, K. Raghavachari, A. Rendell, J. C. Burant, S. S. Iyengar, J. Tomasi, M. Cossi, J. M. Millam, M. Klene, C. Adamo, R. Cammi, J. W. Ochterski, R. L. Martin, K. Morokuma, O. Farkas, J. B. Foresman and D. J. Fox, *Gaussian 09, Revis. D.01*, 2016.
43 Y. Zhao and D. G. Truhlar, *J. Phys. Chem. A*, 2006, **110**, 5121–5129.
44 Y. Zhao and D. G. Truhlar, *J. Phys. Chem. A*, 2006, **110**, 13126–13130.
45 F. Weigend and R. Ahlrichs, *Phys. Chem. Chem. Phys.*, 2005, **7**, 3297–305.
46 D. Andrae, U. Häußermann, M. Dolg, H. Stoll and H. Preuß, *Theor. Chim. Acta*, 1990, **77**, 123–141.
47 O. A. Vydrov and G. E. Scuseria, *J. Chem. Phys.*, 2006, **125**, 234109.
48 O. A. Vydrov, G. E. Scuseria and J. P. Perdew, *J. Chem. Phys.*, 2007, **126**, 154109.
49 O. A. Vydrov, J. Heyd, A. V. Krukau and G. E. Scuseria, *J. Chem. Phys.*, 2006, **125**, 74106.
50 S. Grimme, S. Ehrlich and L. Goerigk, *J. Comput. Chem.*, 2011, **32**, 1456–1465.
51 T. H. Dunning Jr, *J. Chem. Phys.*, 1989, **90**, 1007.
52 N. B. Balabanov and K. A. Peterson, *J. Chem. Phys.*, 2005, **123**, 64107.
53 R. a Kendall, T. H. Dunning Jr. and R. J. Harrison, *J. Chem. Phys.*, 1992, **96**, 6796.
54 D. Figgen, K. A. Peterson, M. Dolg and H. Stoll, *J. Chem. Phys.*, 2009, **130**, 164108.
55 K. A. Peterson, D. Figgen, M. Dolg and H. Stoll, *J. Chem. Phys.*, 2007, **126**, 124101.
56 S. Boys and F. Bernardi, *Mol. Phys.*, 1970, **19**, 553–566.
57 I. D. MacKie and G. A. DiLabio, *J. Chem. Phys.*, 2011, **135**, 134318.
58 D. L. Bergman, L. Laaksonen and A. Laaksonen, *J. Mol. Graph. Model.*, 1997, **15**, 301–306.
59 J. S. Murray, Z. P.-I. Shields, P. Lane, L. Macaveiu and F. A. Bulat, *J. Mol. Model.*, 2013, **19**, 2825–2833.

Published on 01 May 2018. Downloaded by University of New England on 01/05/2018 12:59:59.

Physical Chemistry Chemical Physics Accepted Manuscript

This journal is © The Royal Society of Chemistry 20xx